Theoretical and Applied Climatology
https://doi.org/10.1007/s00704-023-04794-6

RESEARCH

Growing season convective systems in the US Corn Belt in relation to land use-land cover and synoptic patterns

Mikael P. Hiestand[1] · Andrew M. Carleton[1] · Guido Cervone[1,2,3]

Received: 12 July 2023 / Accepted: 8 December 2023

Abstract
Localized short-period studies suggest that differences in surface heat fluxes between croplands and remnant forests of the US Corn Belt—the dominant land use-land cover (LULC) types—influence convective cloud formation in the warm season, primarily around crop-forest boundaries. However, an investigation on interannual timescales is needed to help improve understanding of convective climate in relation to LULC. We use spatial cluster analysis to compare convective systems (CS) from the International Satellite Cloud Climatology Project's Deep Convection Tracking Database to a cropland LULC database for the summer growing seasons (May 1–September 30) of 1999–2007. Spatial–temporal patterns of CS are analyzed with respect to sub-season phenology and LULC type from the National Land Cover Database, and synoptic pressure patterns. The findings indicate two statistically significant clusters of Corn Belt CS; one over the central croplands and the other around crop-forest boundaries in the southeastern area. The clustering of CS, while varying in frequency, remains spatially consistent across sub-seasons and synoptic types. These results suggest a consistent influence of LULC on CS in the Corn Belt that is modulated by synoptic type to either suppress (e.g., via synoptic-scale subsidence) or enhance (via mid-tropospheric upward vertical motion) the frequency of convective clouds and cloud systems. These LULC-related CS clusters are likely the result of non-classical mesoscale circulations originating from spatial contrasts in the surface energy budget and surface roughness between cropland and remnant forests. This study's results will help inform future anticipated modeling projects required to determine these hypothesized LULC-synoptic mechanisms.

1 Introduction

Spatially varying patterns of soil moisture and vegetation resulting from differences in land use–land cover (LULC) types lead to contrasting flux patterns of latent and sensible heat which in turn can fuel deep convection (Pielke 2001). Early modeling studies suggested that widely separated bands of trees planted in areas of otherwise short vegetation increase deep convection (Anthes 1984), through the formation of mesoscale circulations that closely resemble sea breezes (Segal et al. 1988). These non-classical mesoscale circulations (NCMCs) were further linked to spatial heterogeneities in the sensible heat flux (H) and evapotranspiration in addition to differences between contrasting vegetation (Segal and Arritt 1992) and are also known as vegetation breezes (McPherson 2007). The greater height of trees increases their aerodynamic roughness, leading to increased turbulence in the boundary layer and correspondingly higher rates of evaporation, vertical motion, and—under suitable synoptic conditions—precipitating clouds (Blyth et al. 1994). Furthermore, soil moisture boundaries can trigger NCMC formation (Brown and Arnold 1998; Taylor et al. 2007; Frye and Mote 2010). These vegetative and soil moisture boundaries across LULC types serve as foci for mesoscale surface convergence that leads to the initial vertical motion triggering convection (Garcia-Carreras et al. 2011). Additional modeling work shows that surface contrasts between LULC types on length scales of at least 5 km and with low background wind speeds can allow for a transition from shallow cumulus clouds to deep convection (Lee et al. 2019).

✉ Mikael P. Hiestand
mph21@psu.edu

[1] Department of Geography, The Pennsylvania State University, 302 Walker Building, University Park, State College, PA 16802, USA

[2] Institute for Computational Data Sciences, 224 Computer Building, University Park, State College, PA 16802, USA

[3] Earth and Environmental Systems Institute, 2217 Earth-Engineering Sciences Building, University Park, State College, PA 16802, USA

Published online: 28 December 2023

For an NCMC to develop, atmospheric conditions must be favorable in terms of the synoptic circulation, the convective available potential energy (CAPE; Blanchard 1998) and the presence of low convective inhibition (CIN; Trapp 2013). Generally, a weak synoptic (background) airflow is considered favorable for NCMC formation (Avissar and Schmidt 1998), while synoptic scale subsidence can suppress NCMCs (Weaver 2004). However, NCMCs can still occur within larger synoptic circulations (Weaver 2004) that carry them away from the LULC boundaries on which they were initiated (Roy and Avissar 2002; Garcia-Carreras et al. 2010). Additionally, Huang et al. (2022) found that NCMCs form preferentially when large amounts of CAPE are present with warm southerly surface winds in relation to a high-pressure ridge. CAPE is derived by integrating an air parcel's buoyancy between the level of free convection (LFC) and its equilibrium level and can be used to evaluate the potential for convection to occur from near-surface forcing. Conversely, CIN denotes the quantity of work required to initially lift an air parcel past its LFC (Blanchard 1998) and can suppress convective rainfall, potentially leading to drought conditions (Myoung and Nielsen-Gammon 2010; Gerken et al. 2018a). However, the LULC-induced mesoscale updrafts associated with NCMC formation can potentially overcome CIN, allowing sustained deep convection to begin (Garcia-Carreras et al. 2011). These atmospheric conditions favorable to NCMC development occur frequently over the US Corn Belt (Carleton et al. 2008a) and call for more research into land–atmosphere interactions there.

Within the USA, research into land–atmosphere convective interactions typically focuses on the Great Plains (Collow et al. 2014; Huber et al. 2014; Gerken et al. 2018b). Satellite-image studies for that region suggest that deeper clouds tend to develop earlier in the day over agricultural lands than over remnant forests (Adegoke et al. 2007), although there is a dependence on the atmospheric humidity conditions (Rabin et al. 1990). However, the formation of larger convective mesoscale circulations depends upon the amplitude of the surface heat flux (Avissar and Schmidt 1998), with sea breeze–like circulations forming when the amplitude of the surface heat flux variation is sufficiently large (Kang and Davis 2008). East of the Great Plains, the predominant Corn Belt LULC types show similar spatial contrasts in surface roughness and heat fluxes that potentially allow for the LULC-triggered convection to occur (Carleton et al. 1994, 2001).

Within the humid lowland region of rain-fed agriculture in the Midwest USA that stretches from eastern Iowa to western Ohio, or central Corn Belt (Fig. 1), extensive cropland (corn, soybeans) and remnant forest dominate the LULC (Hiestand and Carleton 2020). We hypothesize that, during the warm season, these contrasting LULC types influence convective cloud formation and resulting precipitation. For example, satellite data analysis shows the suppression of convective clouds during the 1988 drought in relation to moisture-stressed crop vegetation—indicated by low values of the Normalized Difference Vegetation Index (NDVI; Xie et al. 2008)—compared to both the adjacent forested areas and also for the non-drought year of 1987 (Carleton et al. 1994). Subsequent satellite-based analysis for the Corn Belt shows that crop-forest boundaries (CFBs) have greater convective cloud development on average compared to the more

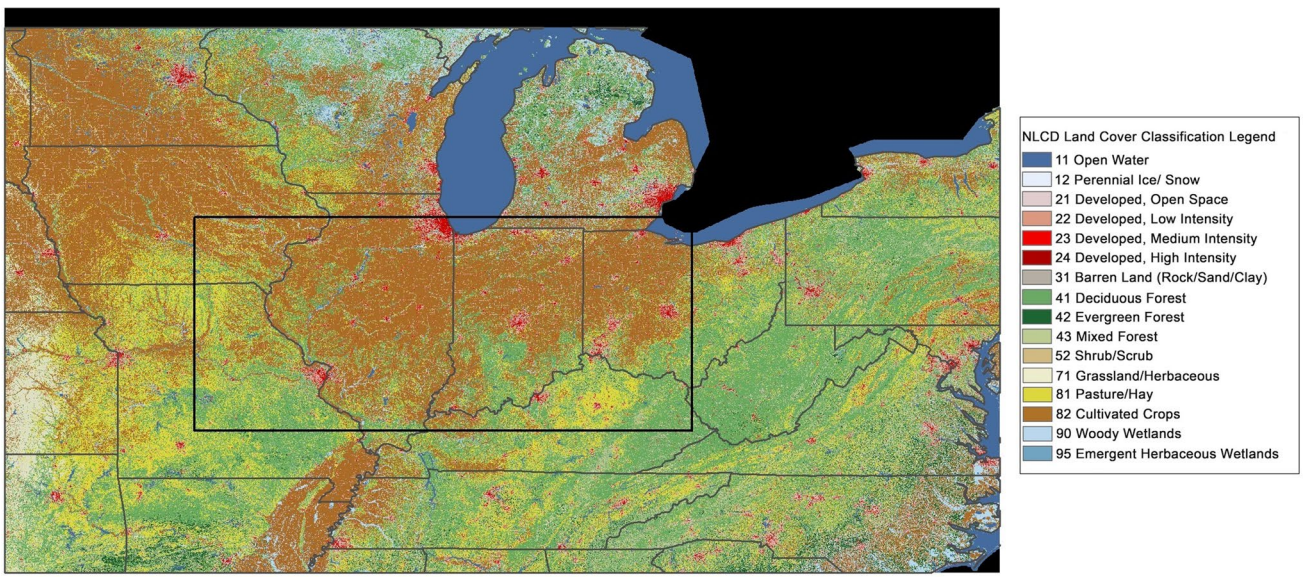

Fig. 1 Land use/land cover map centered on the Midwestern USA. The central Corn Belt study area is contained within the black rectangle. Land-cover data are from the 2004 National Land Cover Database (Yang et al. 2018)

homogeneous crop and forest covers on either side (Carleton et al. 2001). These results suggest that Corn Belt deep convection may be associated with NCMCs around LULC boundaries, similar to those identified in other, mostly drier regions (Segal and Arritt 1992; Carleton et al. 2008b). Furthermore, differences in moisture pooling (the convergent lifting of moist air along CFBs resulting from the contrasting surface roughness) have been hypothesized to enhance deep convection through the lofting of air parcels above the LFC (Carleton et al. 2008a; Matyas and Carleton 2010). However, Corn Belt CFBs appear more likely to trigger deep convection under the specific synoptic conditions of southerly low-level winds, upwards vertical motion both at the surface and in the mid-troposphere, and weak winds aloft (Carleton et al. 2008a). Interestingly, the most recent multi-year satellite analysis (1991–1999) of convective cloud formation in relation to Corn Belt LULC found similar patterns of development in convective clouds over crops, forests, and CFB, at least as determined from daily changes in planetary albedo across nine focused target areas within the Corn Belt (Allard and Carleton 2010).

Other research examining LULC characteristics influencing Corn Belt convection emphasized the importance of both soil moisture and vegetation. For example, Matyas and Carleton (2010) showed that contrasting moist and dry soils in the Corn Belt can enhance convective precipitation similar to other studies conducted for the Midwestern USA (Alfieri et al. 2008) and Oklahoma (Ford et al. 2015). In the Corn Belt, soil moisture correlates positively with NDVI for both cropland and forest LULC types (Adegoke and Carleton 2002), emphasizing the complex relationships among soil moisture and vegetation parameters such as leaf area index (LAI), and phenological stage (Carleton and O'Neal 1995). However, more recent work suggests that the lower-atmosphere humidity displays a stronger coupling with Corn Belt convective precipitation than does soil moisture (Chapman and Carleton 2021), potentially highlighting the importance of LULC-influenced moisture pooling (Carleton et al. 2008a). Consequently, further investigation is needed to determine more fully the presence and character of interannual spatial relationships between CFBs and convective cloud formation in the central Corn Belt region.

The analysis of surface heat fluxes from two flux towers, each representative of cropland and remnant deciduous forest for the growing seasons of 1999–2007 (Hiestand and Carleton 2020), showed that the site differences in sensible (H) and latent (LE) heat are greatest when the synoptic atmospheric pattern comprises a low-pressure system to the west and high-pressure system to the east of the Corn Belt, giving a humid southerly wind flow. Additionally, croplands and forests display contrasting responses in their LE and H fluxes related to their phenological stage. The forest areas dominate the LE flux at the start of the growing season (early May to mid-June) when the croplands exhibit the higher H flux. However, during the middle to late growing season (mid-June to August), this pattern reverses: the croplands have higher LE, while the forest has a higher H flux (Hiestand and Carleton 2020). The importance of phenology on Corn Belt surface heat fluxes is further illustrated by significant sub-seasonal variations in LE and H from croplands and deciduous forests that are lost in averaging over longer time scales (Hiestand et al. 2023). The magnitude of the heat fluxes and their identified differences according to LULC type, sub-season phenology, and synoptic circulation type ("Synoptic Type" hereafter), are likely also evident in the spatial patterns of convective cloud activity.

Accordingly, we hypothesize (1) that convective systems will cluster around CFBs in the Corn belt, (2) that the clustering of CS around CFBs will vary with respect to subseason and synoptic circulations, and (3) that some of the convective systems may be indicative of NCMCs. Therefore, this paper determines the 9-year (1999–2007) spatial patterns of convective cloud formation in relation to Corn Belt LULC by identifying the presence of statistically significant clusters of convective systems from the International Satellite Cloud Climatology Project (ISCCP) dataset (Schiffer and Rossow 1985, 1983). Specifically, the ISCCP's Deep Convection Tracking Database (DCTD) is used in relation to Corn Belt LULC information from the US National Land Cover Database (NLCD; Jin et al. 2019) to identify convective systems in relation to prevailing synoptic type and time within the growing season (related to phenology). More specifically, we determine (i) where convective clouds form in relation to CFBs and their possible association with synoptic pressure patterns over the Corn Belt, and (ii) whether convective clouds are associated more strongly with LULC during the start, middle, or end periods of the summer growing season. This approach differs from that taken by Allard and Carleton (2010) in that we employ a spatial cluster analysis in the form of local Moran's I to identify spatial relationships between convective systems and high-resolution LULC data across the Corn Belt. Additionally, we use data from the North American Regional Reanalysis (NARR; Mesinger et al. 2006) to investigate the likelihood that convective systems around the CFB are related to NCMCs. From the results of the statistical cluster analysis, we infer candidate physical mechanisms as hypotheses to be investigated in anticipated modeling studies.

2 Methods

2.1 Study area and time period

This analysis is undertaken for the region extending from western Ohio westward into eastern Iowa and south into

Southern Illinois, or the central Corn Belt (Fig. 1). This region omits Nebraska and Iowa, which are occasionally considered part of the Corn Belt but climatically resemble the Great Plains region (Hiestand and Carleton 2020). This study consists of the nine summer growing seasons May 1st through September 30th of 1999–2007. To investigate the sub-seasonal associations of convective clouds with LULC, the growing season is divided temporally into three broad phenological stages representative of the biophysical development of both LULC types (cropland, forest), as follows: the start of growing season (SOGS: May 1st through June 20th), middle of growing season (MOGS: June 21st through August 10th), and end of growing season (EOGS: August 11th through September 30th). This seasonal sub-division is the same as used in Hiestand et al. (2023).

2.2 Convective cloud data and analysis

The ISCCP DCTD provides a reliable climatological dataset to analyze deep convective clouds for the 1999–2007 growing seasons. Here a convective cloud is defined by having an infrared brightness temperature below 245 K (Machado et al. 1998). Starting in 1982, ISCCP combines cloud data from a variety of satellite platforms to create an ongoing, long-term global cloud climatology (Rossow et al. 2022). The ISCCP algorithm analyzes differences in coincident infrared and visual radiances to differentiate between cloudy, mixed, and clear pixels (Rossow and Garder 1993). Here, DCTD data from GOES-E (75°W), which obtains better views of the Corn Belt than GOES-W (135°W), are used to identify convective clouds based on their low infrared brightness temperature (T_{IR}) (Machado et al. 1992). The ISCCP DCTD data are available online at https://isccp.giss.nasa.gov/CT/.

First, a convective system (CS) is determined from a cloud-top temperature threshold of less than 245 K and then tracked in 3-h time steps to identify a subsequent convective cluster (CC) having a cloud-top temperature of less than 218 K. The CC signifies the core of the convective cell within the CS and can either represent precipitating (i.e., deep convection) or non-precipitating clouds (Machado et al. 1998). In this study, we select Corn Belt CS that occur during the 1100–1900 LST window, when surface forcing from solar heating is most likely to trigger convection (Hiestand and Carleton 2020). Then, we map the centers of the CS as points that are plotted over the fuzzy CFB map (see below) to determine where deep convection initiates and its statistical associations (local Moran's I) with the LULC. Last the mapped spatial cluster results from local Moran's I are used to infer the likely physical processes involved, including NCMCs.

2.3 Land use-land cover data and their analysis

To determine the locations of the cropland and remnant forest LULC types within the Corn Belt we use the National Land Cover Database (NLCD) for the year 2004, which is the approximate mid-point of the study period. The NLCD is derived from USGS Level-1 Landsat data at a spatial resolution of 30 m (Jin et al. 2019) and is available through the multi-resolution land characteristics (MRLC) consortium at https://www.mrlc.gov/data. To divide the Corn Belt into homogeneous cropland and forest LULC types, the NLCD "Pasture/Hay" and "Cultivated Crops" LULC types are first combined into one generic crop category, and the "Deciduous Forest", "Evergreen Forest", and "Mixed Forest" are combined into a generic forest LULC category, using RStudio. Merging several LULC types into larger LULC categories is consistent with past research into land surface-climate associations in the Corn Belt (Allard and Carleton 2010; Carleton et al. 2008b; Matyas and Carleton 2010). Our approach expands on these past studies by using high-resolution LULC data to generate a "fuzzy" CFB map that indicates the geographic location of CFBs while also depicting a transition or border zone between crops and remnant forests.

To create the fuzzy CFB map for statistical comparison to CS locations, the generic forest pixels are assigned a value of zero, and the generic crop pixels are assigned a value of 1. The fuzzy CFB is derived by conducting a 15-km (501×501 pixels) moving-window spatial average around each LULC pixel, following sensitivity testing with 2-km, 5-km, and 10-km moving averages that produced broadly similar locations of the CFBs. The 15-km moving average was selected as it depicts a border zone at the scale at which LULC is likely to influence NCMCs (Carleton et al. 2008b). The moving spatial average results in each pixel receiving a decimal value ranging between zero and one, with pixels closest to the CFB having a border score that approaches 0.5. In the resulting CFB map (Fig. 2), the forest is defined by pixel values between 0 and 0.2, the fuzzy CFB zone has pixel values between 0.2 and 0.8, and cropland is defined with values greater than 0.8. We repeated this spatial moving average procedure for the 2001 and 2006 NLCD data to verify a lack of LULC temporal change in the Corn Belt.

2.4 NARR data

For analyzing Corn Belt CS–LULC associations in the context of the atmospheric near-surface synoptic circulation (air pressure, winds) and its physically relevant variables (e.g., the vertical motion of air, or Omega, and the convective available potential energy, CAPE), we apply the manual synoptic classification developed for this region in Hiestand and Carleton (2020) and Hiestand et al. (2023). This scheme uses manual interpretation of daily-average

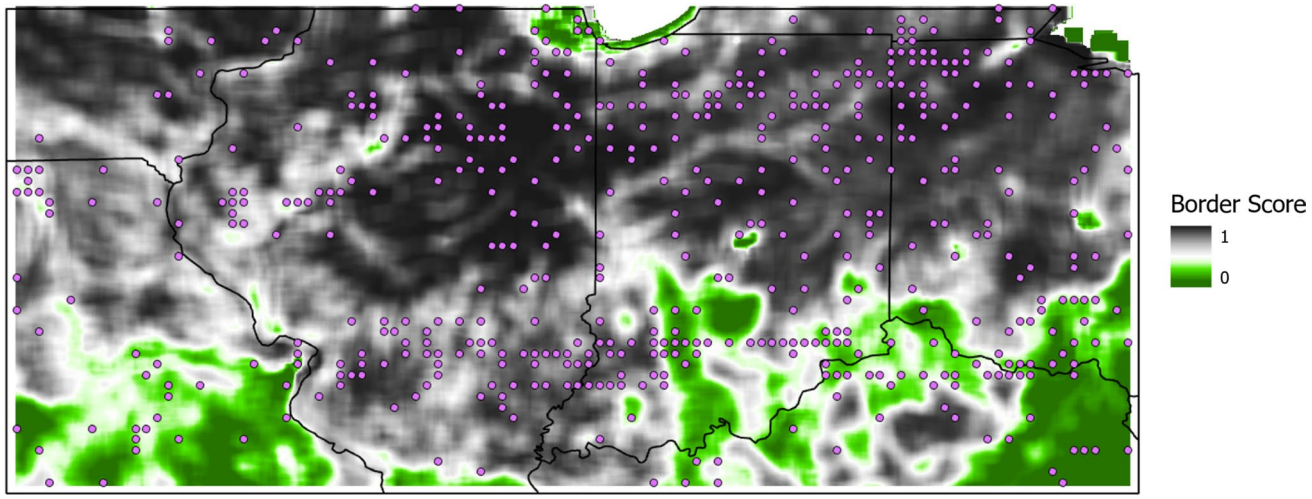

Fig. 2 The center points of all 756 CS (pink circles) overlaid on the fuzzy CFB map of the Corn Belt for growing seasons 1999–2007. Black represents croplands, and green indicates forest areas, while white denotes the fuzzy crop–forest border (CFB) zone

maps of mean sea level pressure and 1000 hPa vector winds from the NARR (Mesinger et al. 2006). The classification consists of seven distinct synoptic types (Table 1). Synoptic type 1 is a high-pressure system centered directly over the Corn Belt, with light anti-cyclonic (i.e., clockwise, divergent) wind flow. Synoptic Type 2 is a low-pressure system centered on the Corn Belt with stronger cyclonic (anti-clockwise, convergent) wind flow. Synoptic type 3—the most common in this study—has a low-pressure center to the west and a high-pressure center to the east of the Corn Belt with a resulting southerly wind flow from the direction of the Gulf of Mexico. Synoptic type 4 has a high-pressure center to the west and a low to the east with resulting northerly flow over the Corn Belt. Synoptic type 5 is a "col" pattern (Fig. 3), also sometimes referred to as a saddle, that consists of opposing high-pressure and low-pressure areas in the corners of the study region and a generally slack wind field with variable wind directions depending on location. Synoptic type 6 has a high to the north and low to the south of the Corn Belt with associated easterly near-surface wind flow, and synoptic type 7 has a low to the north and a high to the south with accompanying westerly wind flow over the Corn Belt.

The frequencies of these synoptic types by growing season in the 1999–2007 period are shown in Table 2. All NARR data are available online from the NOAA/OAR/ESRL Physical Science Division at https://psl.noaa.gov/cgi-bin/data/narr/plotday.pl/. To identify possible associations of Corn Belt convective cloud activity with the daily (May through September) environment of vertical motion above the planetary boundary layer (e.g., Carleton et al. 2008b), we also use the NARR daily average data to determine the mid-tropospheric (500 hPa) omega field, where negative values indicate ascending air and positive values indicate descending air (i.e., subsidence). For atmospheric variables at or near Earth's surface that are potentially representative of a physical association between convective clouds and LULC (Carleton et al. 2008b), we use NARR daily average data for the 1000 hPa omega field and CAPE, which is also composited separately by individual growing season and synoptic type.

Table 1 Summary of the seven synoptic types developed by Hiestand and Carleton (2020) along with their associated wind flow regimes and generalized weather patterns

Synoptic type	Synoptic pressure pattern	Wind regime	Associated weather
1)	High over Corn Belt	Anticyclonic, light	Fair with light variable winds
2)	Low over Corn Belt	Cyclonic, strong	Showers/T-storms with variable winds
3)	Low to the West, high to the East	Southerly	Mostly cloudy with scattered showers
4)	High to the West, low to the East	Northerly	Partly cloudy with isolated showers
5)	Col system of alternating highs and Lows	Weakly Convergent	Cloudy with isolated or scattered showers
6)	High to the North, low to the South	Easterly	Cloudy to partly cloudy
7)	Low to the North, high to the South	Westerly	Fair to party cloudy

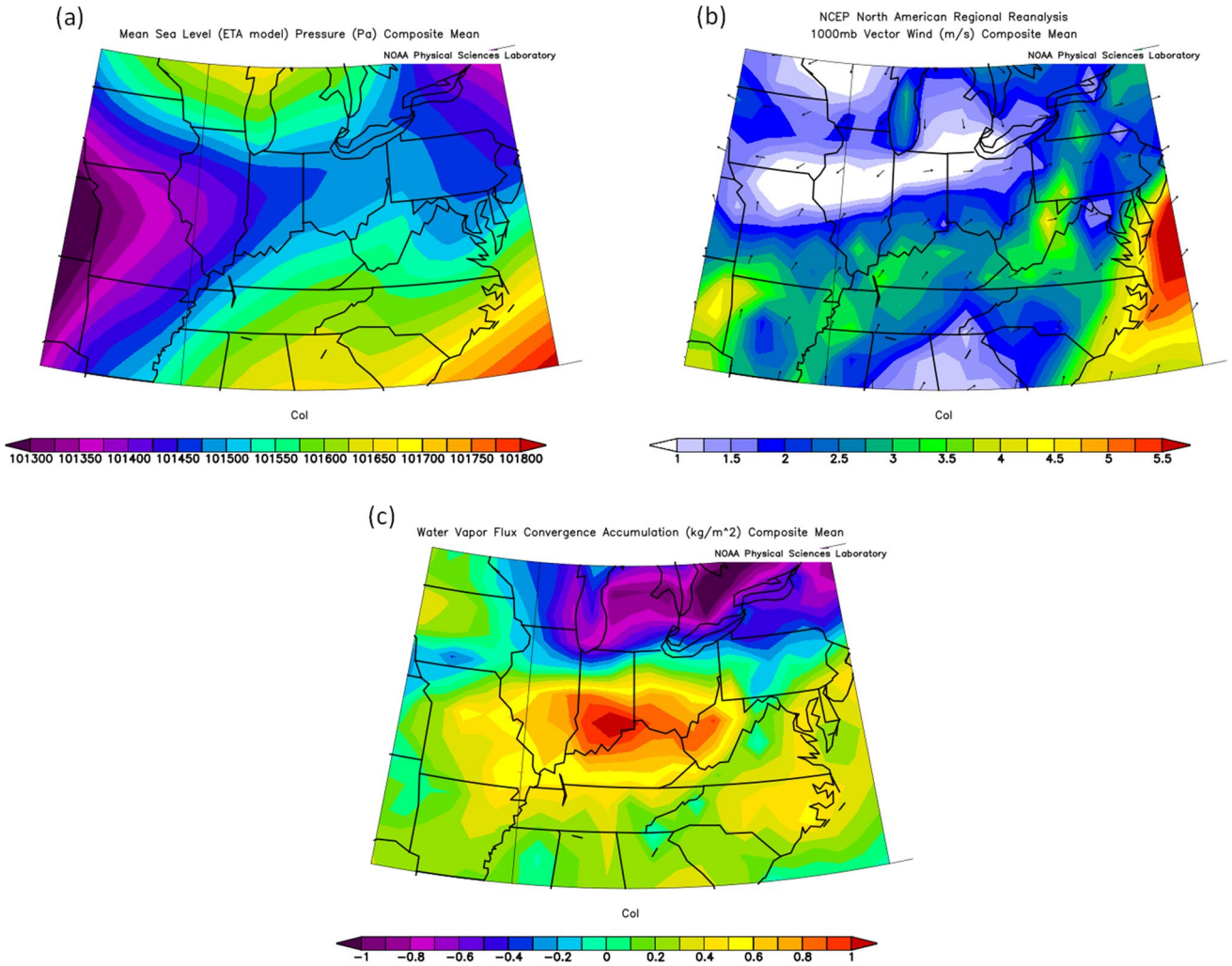

Fig. 3 Composite images showing the synoptic type 5 pattern **a** mean sea level pressure (Pa), **b** 1000 hPa vector wind field (m/s) indicating surface convergence, and **c** water vapor flux convergence accumulation (kg/m^2) over the Corn Belt

Table 2 The frequency of each synoptic type for summer growing seasons of 1999–2007 (from Hiestand and Carleton 2020)

Growing season synoptic classification counts										
Synoptic type	1999	2000	2001	2002	2003	2004	2005	2006	2007	Total
1)	14	15	16	19	9	14	12	13	15	127
2)	8	13	9	4	9	2	7	9	5	66
3)	53	63	51	61	44	64	61	52	63	512
4)	18	14	17	9	19	26	11	20	16	150
5)	13	11	9	12	14	13	9	15	10	106
6)	15	19	23	37	35	14	31	24	30	228
7)	32	18	28	11	23	20	22	20	14	188

2.5 Cluster analysis of convective systems

In determining the presence of statistically significant clusters of CS in relation to the fuzzy CFB map, we use local Moran's I (Anselin 1995). Local Moran's I determines if significant (i.e., non-random) spatial clustering is present, and can also be used to show the physical locations of statistically significant clusters of cloud systems (Park et al. 2018). Unlike other forms of spatial pattern analysis, such as Getis-Ord Gi* (Getis and Ord 1992) which requires setting predefined distance thresholds (Rossi and Becker 2019), or chi-squared (McHugh 2013) which would require grouping

the data into grid squares, local Moran's I (Anselin 1995) does not require any arbitrary groupings of the CS. First, the center points of all CS contained in the DCTD are overlaid on the 2004 fuzzy CFB map and assigned a numerical border score from the fuzzy CFB map ranging from 0 (forest) to 1 (cropland), with decimal values indicating CFB pixels. Then, every CS with a border score greater than 0.5 is rescaled by subtracting one and then multiplying by − 1 to put each CS border score on a scale from zero 0.0 to 0.5, where 0.0 indicates that a CS is not in a fuzzy CFB zone and 0.5 indicates the center of a fuzzy CFB zone. Local Moran's I is then applied to the CS point data to determine the locations of significant CS clusters in relation to CFBs. The CS data are also subset by synoptic type and sub-season for individual testing with local Moran's I to create a series of maps showing the distribution of significant clusters of CS over the fuzzy CFBs zones, croplands, and forests.

3 Results and discussion

3.1 Fuzzy LULC map

The fuzzy LULC map is shown in Fig. 2. The moving spatial mean smoothes over pixels of missing data and other LULC types (such as urban areas) to create a continuous raster with values ranging from 0 (forest) to 1 (cropland). Decimal values that approach 0.5 indicate raster cells that are closest to the actual CFB where croplands adjoin forested areas. Any raster cell with a value between 0.2 and 0.8 is within the fuzzy CFB zone. The percentage of total Corn Belt area of forests, CFBs, and cropland LULC types for the 2001, 2004, and 2006 NCLD data (Table 3) remain broadly consistent across the study period, although there was a slight increase (+ 0.05%) in forested area between 2004 and 2006 at the expense of the CFB. This minimal change in LULC cover between 2001, 2004, and 2006 indicates that the distribution of croplands and remnant forest in the Corn Belt is largely static, and thus, changes in LULC do not need to be incorporated into the cluster analysis.

Table 3 The percentage for Corn Belt area covered by each of the three LULC types on the fuzzy CFB maps for the 2001, 2004, and 2006 NLCD data

Percent area for fuzzy border maps			
LULC type	2001	2004	2006
Forest	1.04	1.00	1.05
Border	41.53	42.26	42.16
Crop	57.43	56.74	56.79

3.2 Statistical Clustering of CS for the 1999–2007 Growing and Sub-Seasons

A total of 756 CS occurred over the study area for the 1999–2007 growing seasons. Of those, 35 (4.6%) occur over the forest (i.e., border score less than 0.2), 284 (37.6%) occur in the CFB (border score between 0.2 and 0.8), and 437 (57.8%) occur over the croplands (border score greater than 0.8). The center point locations of all 756 CS overlaid on the fuzzy CFB map for 2004 (Fig. 2) show a high degree of spatial autocorrelation, where statistically significant clusters of CS occur over all three LULC groups. Cluster analysis of each CS and its matching convective cluster (CC) center produces similar results, as a CC represents the same CS three hours later and shows minimal movement over that period. Therefore, the spatial patterns of CC are not discussed further here.

The spatial distribution of CS significant clusters for all nine growing seasons, as determined by local Moran's I, is shown in Fig. 4. These clusters indicate regions where the groupings of CS are unlikely the result of chance and express a statistically significant spatial (but not necessarily causal) relationship between CS and LULC. Clusters are indicative of LULC type with "low" clusters indicating cropland or forest and "high" clusters representing CFBs. Significant outliers indicate that a CS is part of a larger cluster but that the CS has a border score notably different from that of the surrounding CS within the same cluster, producing "High-Low" outliers over CFBs and "Low–High" outliers over cropland or forest. A large statistically significant cluster occurs over croplands in the northern Corn Belt stretching from central Illinois to eastern Ohio (Fig. 4), with nine significant outliers over CFBs that represent CS which are part of the cropland cluster but have border scores indicating that they are near a CFB. The CFBs exhibit separate significant clusters of CS formation in northern and central Missouri, eastern and central Illinois, and across southern Indiana and Ohio into northern Kentucky. The forest land cover shows only one significant cluster of CS, over eastern Kentucky; however, there are 13 CS over forest areas in the Corn Belt that are statistically significant outliers surrounded by significant clusters of CS over CFBs. There are seven CS occurring over croplands that are significant outliers, meaning that they have low border scores compared to their neighboring CS over CFBs, indicating that their location over croplands is unlikely due to random chance and they are still part of a statistically significant cluster occurring mostly over CFBs.

These novel results of CS cluster locations emphasize the importance of considering the Corn Belt in its entirety when studying interannual LULC interactions with deep convection. Using data from across the Corn Belt uncovers previously unidentified regions of CS development that fall outside of the target areas employed in Allard and Carleton

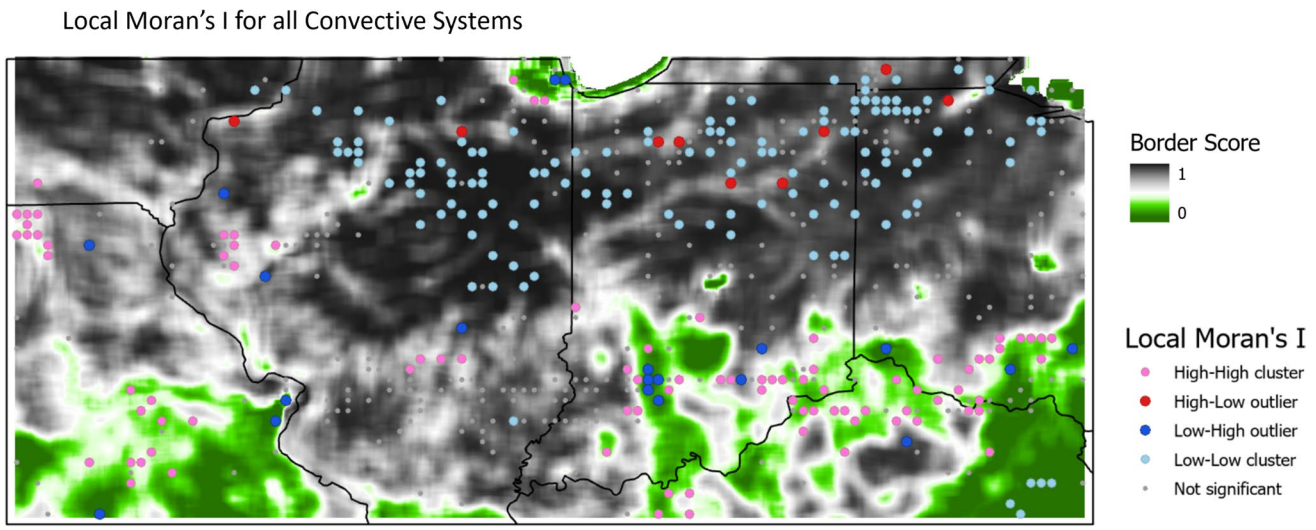

Fig. 4 Results from local Moran's I for CS (total = 756) in the US Corn Belt for the 1999–2007 growing seasons. Pink dots indicate a statistically significant cluster of CS with a high border score, light blue dots indicate a statistically significant cluster of CS with a low border score (i.e., cropland or forest), red dots indicate a statistically significant outlier with a high border score, and dark blue dots indicate a statistically significant outlier with a low border score (cropland or forest). Grey dots are non-significant CS

(2010). Notably, these new areas of interest include the large cluster of CS over the croplands and the cluster of convective systems over CFBs in the southern Corn Belt. Furthermore, the CS cluster over the CFB seems to confirm the hypothesis presented by Carleton et al. (2008b) that LULC is influencing convective development around CFBs. However, establishing a causal relationship between CFBs and CS development will require numerical modeling experiments that are outside the scope of the current study.

3.3 Sub-seasonal patterns in CS clustering

All three phenological sub-seasons (Fig. 5) show a spatial clustering in CS broadly similar to that for the whole growing season. However, the main difference among sub-seasons is that the number of CS decreases from the SOGS to the EOGS (Table 4). For the SOGS, there is a large and significant CS cluster over croplands in the northern Corn Belt, while the CFBs show three significant clusters of CS in the eastern Corn Belt and a large significant cluster in the southeastern Corn Belt (Indiana, Kentucky, and Ohio). Additionally, the SOGS has four significant CS outliers over CFBs, and five significant outliers each over forests and croplands (Fig. 5).

During the MOGS there are 13 CS over forests, 75 CS over CFBs, and 121 CS over croplands. This sub-season has two significant CS clusters over cropland in the northern Corn Belt and a significant cluster over the CFBs in the southeastern Corn Belt, indicating strong spatial autocorrelation among convective systems in those sub-regions. Also, for the MOGS, there are three significant outliers over the CFB, four over the croplands, and one over the forest (Fig. 5), indicating CS that are part of a cluster but have a different border score than the other CS within the same cluster. During the EOGS, there are six CS clusters over the forests, 67 over the CFBs, and 80 over the croplands. For this same sub-season, there is a significant cluster of CS over croplands in the northern Corn Belt and a smaller significant cluster over the CFBs in southern Indiana. The EOGS has two significant outliers over the CFBs and three each over croplands and forested areas.

For all three sub-seasons considered together, the Corn Belt shows similar spatial distributions in the two main significant clusters of CS initiation: over the northern croplands, and at the CFBs. This spatial pattern of CS clusters suggests a strong and consistent influence of LULC on Corn Belt CS. However, there is a decrease in the total number of CS—but not the cluster locations—from the SOGS into the MOGS and then the EOGS. This result is consistent with Hiestand and Carleton (2020), who hypothesized that the observed large differences in surface heat fluxes between Corn Belt croplands and deciduous forests are most likely to trigger convection during the SOGS when the trees have higher latent heat fluxes than the immature crops (Hiestand and Carleton 2020). The present result suggests that phenology is not influencing the statistically significant spatial location of CS development but rather the changing frequency of CS across the growing season. One possible explanation for the consistent spatial patterns in CS across the growing season, despite the known phenological switch in LE and H between croplands versus forest, is that there are

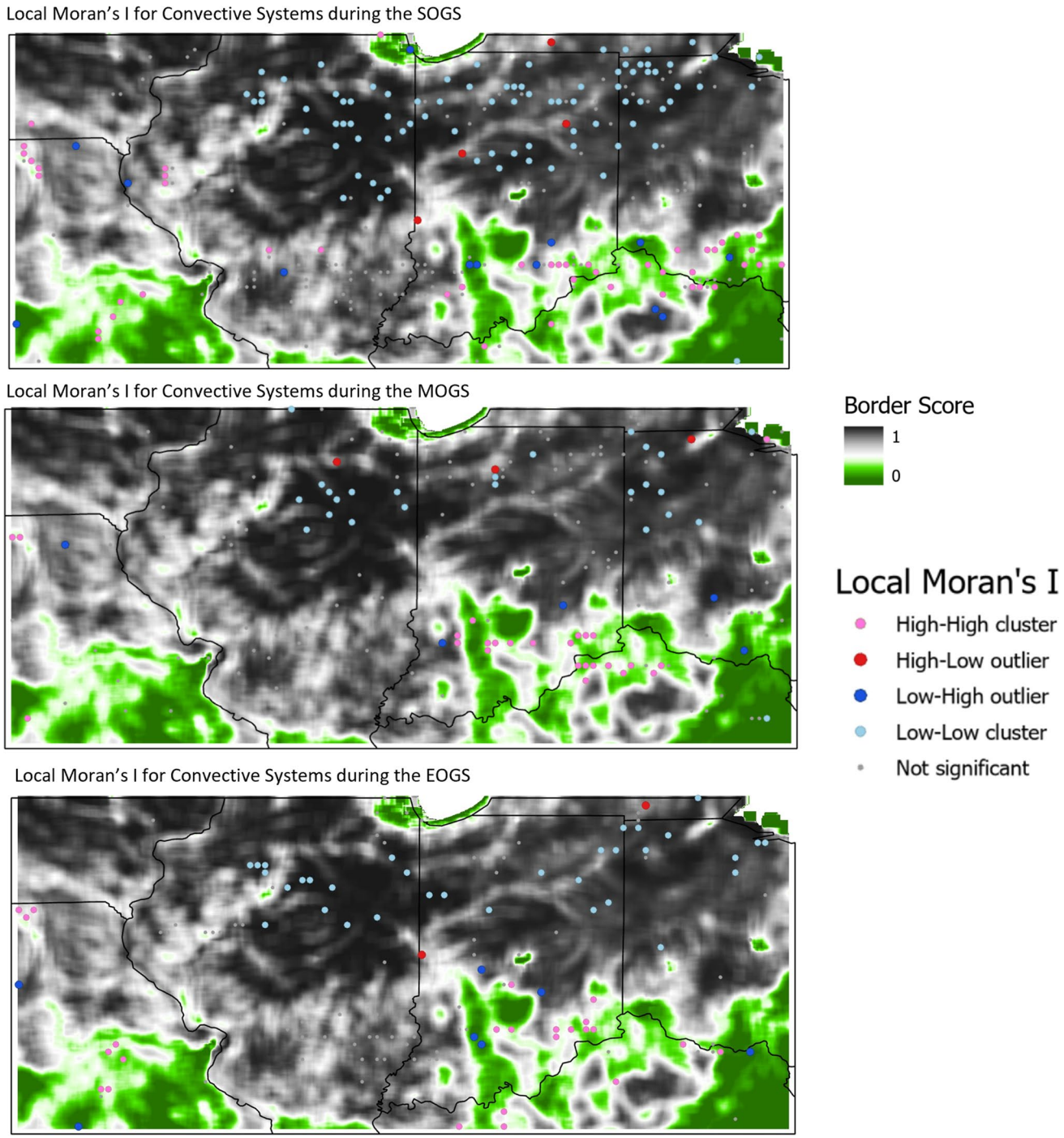

Fig. 5 Similar to Fig. 4, but for separate local Moran's I statistics of CS during the SOGS (top), MOGS (middle), and EOGS (bottom) portions of the 1999–2007 study period

fewer NCMCs in the MOGS and EOGS than the SOGS to drive CS formation around CFBs due to the reduced contrasts in LE and H across the CFB. In the MOGS and EOGS, the crops exhibit higher LE fluxes than the forest, but the magnitude of the difference between the surface heat fluxes is not as strong as in the SOGS when the forests exhibit higher LE fluxes than the crops (Hiestand and Carleton 2020).

Table 4 Number of convective systems (CS) for the 1999–2007 growing seasons and sub-seasons, by LULC type

	Total	Start	Middle	End
Forest	35	16	13	6
Border	284	142	75	67
Crop	437	236	121	80
Total	756	394	209	153

3.4 CS statistical clustering in relation to synoptic types

Under different synoptic types, the CS still have the same broad spatial clustering patterns in relation to LULC as observed for the entire study period (discussed above), but their frequencies and exact locations vary. When an individual synoptic type (e.g., types 3, 5, and 6) has a sufficiently large number of CS to produce statistically significant clusters, those CS tend to occur primarily over crops in the northern Corn Belt with a secondary cluster over CFBs in the southeastern Corn Belt (Figs. 6, 7, and 8). This consistent bimodal pattern suggests that the strong influence of LULC on CS development across sub-seasons, shown above, is also maintained across the range of synoptic types. However, the synoptic pressure patterns and associated winds play a large role in determining the number of CS that develop (discussed below).

When the total number of CS occurring over cropland, CFBs, and forest are stratified by synoptic type (Table 5), the highest frequency by far (379 or 50.1%) is associated with synoptic type 3, comprising a westward low center and eastward high center with southerly near-surface flow over the Corn Belt. These CS exhibit a large and statistically

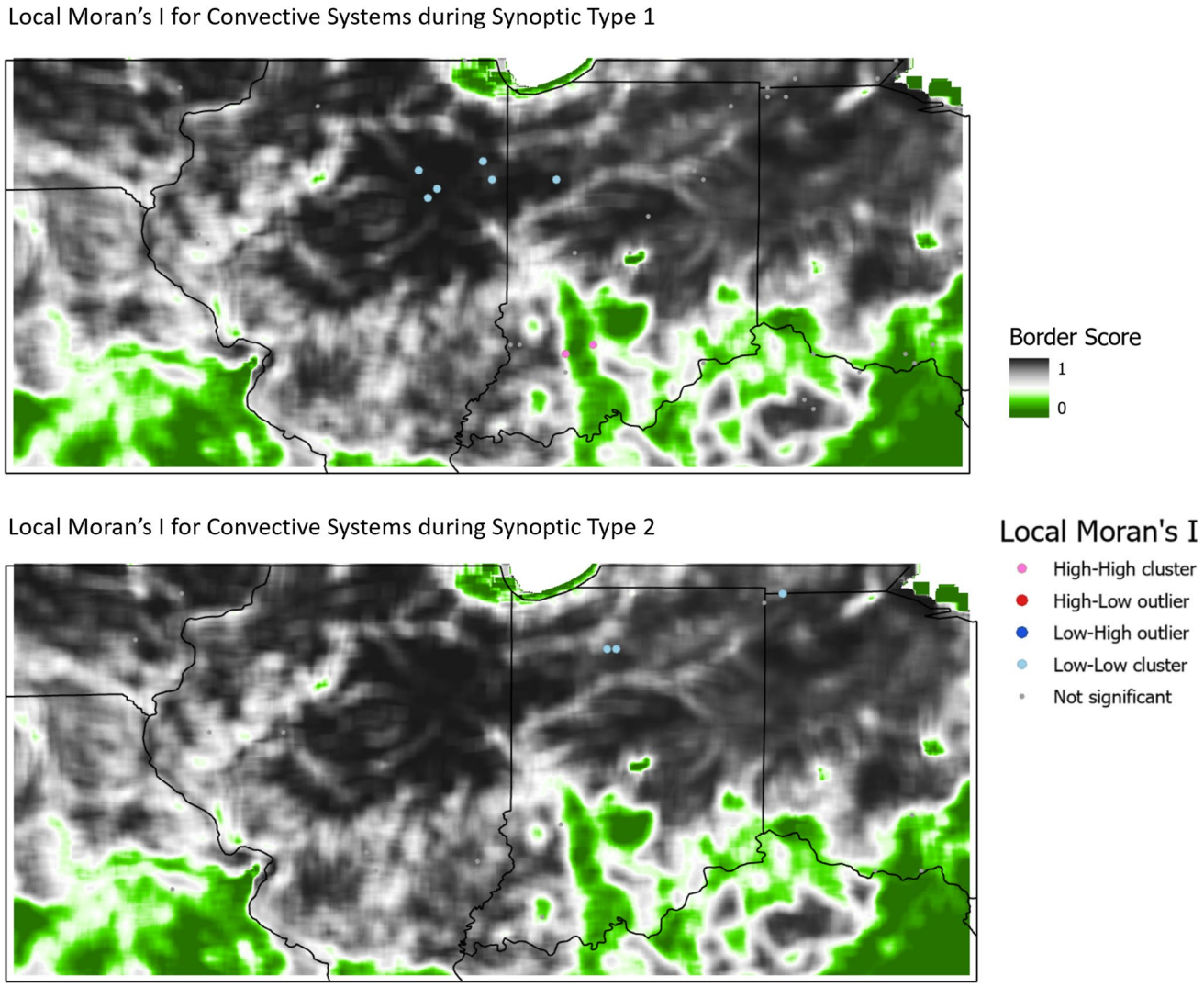

Fig. 6 Similar to Fig. 4 but for separate local Moran's I statistics of synoptic type 1 (top) and synoptic type 2 (bottom)

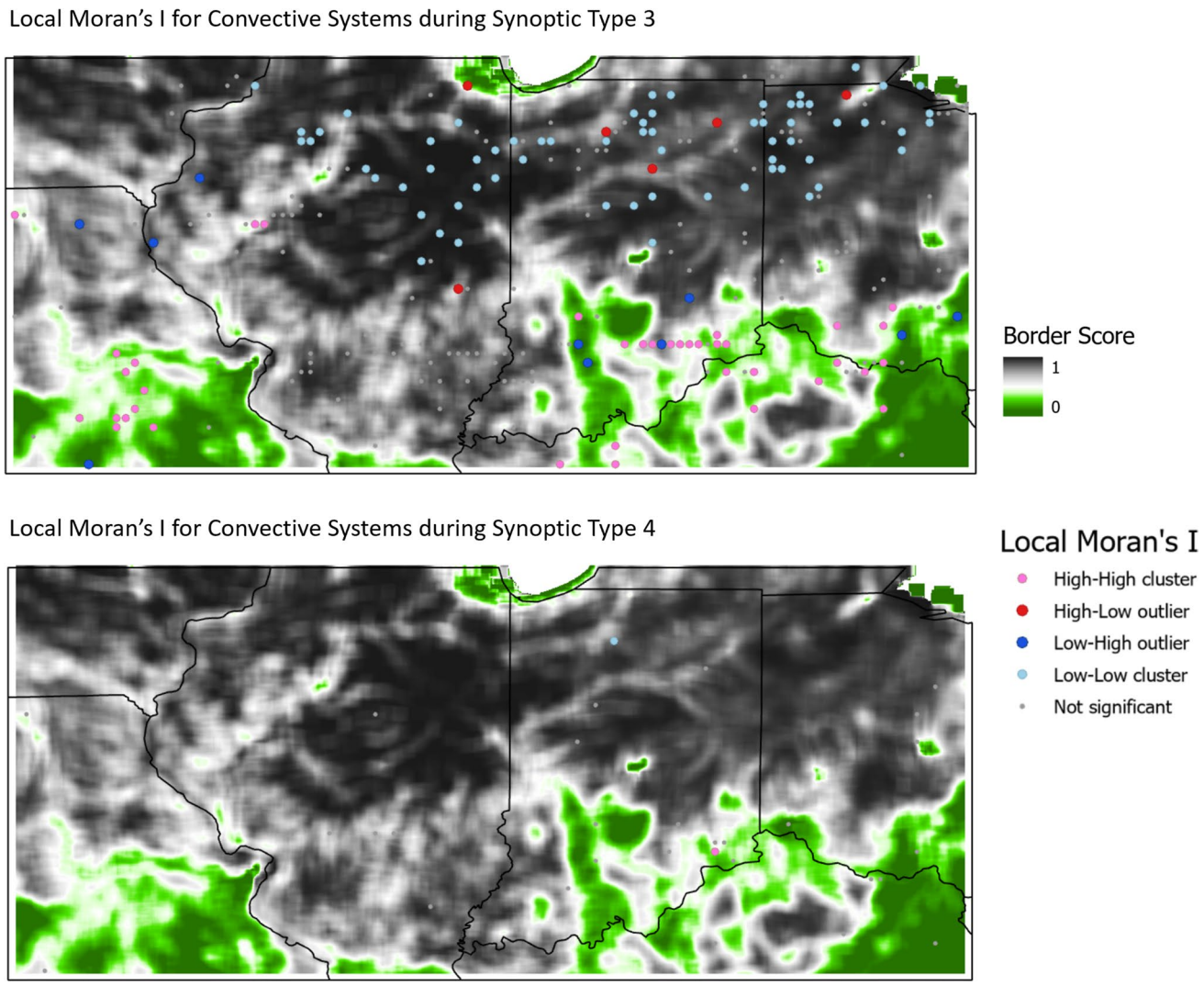

Fig. 7 Similar to Fig. 4 but for separate local Moran's I statistics of synoptic type 3 (top) and synoptic type 4 (bottom)

significant cluster over the croplands in the northern Corn Belt stretching from western Ohio into eastern Illinois, a small significant cluster over the CFBs in central Missouri, and a larger significant CFB cluster in southern Indiana extending into Ohio. Additionally, there are six significant outliers over the CFBs, five over the forest and five over the croplands (Fig. 7). Synoptic type 3 is accompanied by conditions favorable for LULC to trigger atmospheric convection due to high static instability in the moist southerly flow: the surface heat flux differences between cropland and forest are at their greatest during this synoptic pattern and therefore the most likely to trigger vertical air circulations along or near CFBs (Hiestand and Carleton 2020). Additionally, the increased humidity associated with this type, combined with high levels of soil moisture, is conducive to the generation of convective precipitation (Chapman and Carleton 2021).

The synoptic pattern having the second-highest frequency of CS for the study period (146, 19.3%), the type 6 synoptic pattern with a high to the north and low to the south (Fig. 8) with easterly near-surface winds over the Corn Belt, shows the familiar pattern of significant CS clusters over the croplands in the northern Corn Belt and a large significant cluster of CS over the CFB in the southeastern Corn Belt. This result suggests that LULC can influence CS development when cool humid air is advected into the Corn Belt from the east and northeast and destabilized by surface heating.

The third highest frequency of CS (100, 13.2%) is associated with synoptic type 5 (col), which shows a significant cluster over croplands in Illinois and in the CFB in northern Kentucky (Fig. 8). The Illinois cluster approximately coincides with the average eastern position of the warm front in the col pattern that often characterizes type

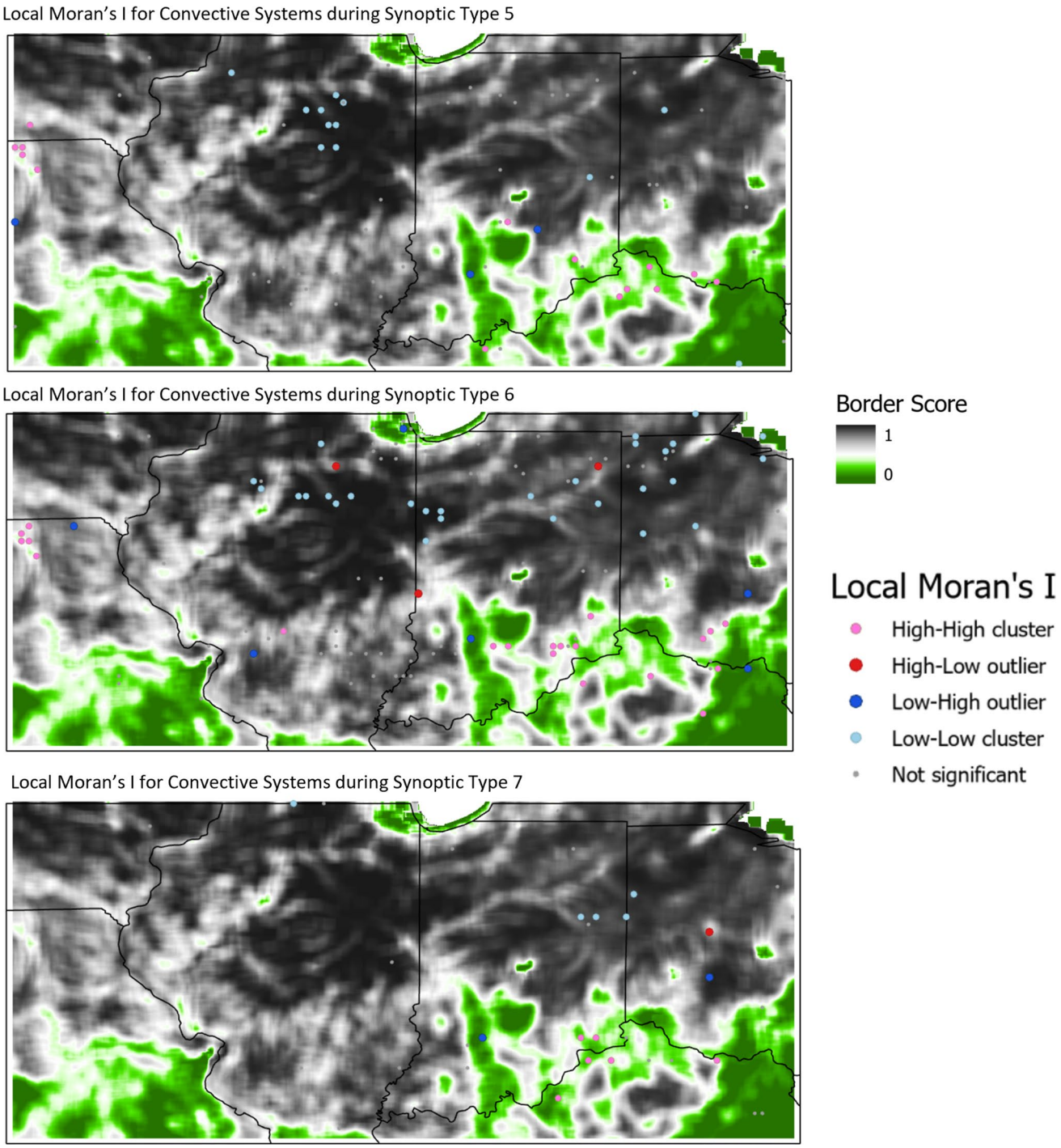

Fig. 8 Similar to Fig. 4 but for separate local Moran's I statistics of synoptic type 5 (top), synoptic type 6 (middle), and synoptic type 7 (bottom)

Table 5 Number of convective systems (CS) by synoptic type for the 1999–2007 growing seasons, stratified by LULC type

	Type 1	Type 2	Type 3	Type 4	Type 5	Type 6	Type 7
Forest	2	1	14	2	7	6	3
Border	11	8	127	19	42	55	22
Crop	25	11	238	9	51	85	18
Total	38	20	379	30	100	146	43

C type

5, accompanied by diminished deep-layer static stability that is characterized by large CAPE values (Fig. 9).

Under synoptic type 7 (Fig. 8) with a low-pressure center to the north and a high-pressure center to the south (43, 5.7%), small significant clusters of CS are located over croplands and the CFB in the eastern Corn Belt. However, there are almost no significant clusters of CS in the west-central Corn Belt accompanying type 7, which is consistent with the relatively cool and dry (i.e., relatively stable) air mass dominating this synoptic pattern.

Synoptic types 1 (high-pressure center directly over the Corn Belt) and 4 (western high and eastern low) both exhibit low frequencies of CS (Table 5), consistent with relatively stable atmospheric conditions and low CAPE (Fig. 9). For synoptic type 1, this involves subsiding air suppressing convective development (Weaver 2004; Hoerling et al. 2014) despite potential surface forcing, and for type 4, the associated cool and dry northwesterly flow likely inhibits CS formation through column shrinking as air acquires anticyclonic vorticity and diverges on the eastern side of the upstream high-pressure system. Interestingly, synoptic type 4 is the only pattern in which the CFB has a higher number of CS than either the croplands or the forested areas, possibly the result of strong contrasts in surface heat fluxes and aerodynamic roughness between cropland and forest. Nevertheless, synoptic types 1 and 4 display similar general patterns of a single small significant cluster of CS in each pattern over the croplands in the northern Corn Belt and over the CFB in the southern Corn Belt (Figs. 6 and 7).

Finally, synoptic type 2 (with a low-pressure center directly over the Corn Belt) has the least CS of any synoptic type (20, 2.7%) and only two small significant spatial clusters (Table 5, Fig. 6). Although heavy cloud cover and precipitation frequently accompany this synoptic type, the algorithm used in the DCTD is optimized to identify mesoscale CS (Machado et al. 1998) rather than the deep convection embedded within frontal (quasi-linear baroclinic) cloud systems. Across all these synoptic types, only 15 of the 756 CS analyzed have a radius greater than 200 km with the single largest CS being 234 km in radius. Accordingly, the synoptic-scale and frontally organized convective events associated with synoptic type 2 fall outside the scope of this paper.

3.5 Influences of CAPE and omega on synoptic type associations with CS

Differences in the composite CAPE patterns between synoptic types (Fig. 9) emphasize the relationship between synoptic conditions and CS resulting from atmospheric instability, as those types with characteristically high CAPE exhibit higher frequencies of CS than those with low CAPE. For instance, synoptic types 3 (379 CS) and 5 (100 CS) with relatively high CAPE (greater than 800 J/kg) over the Corn Belt generate high numbers of CS that form significant clusters in relation to LULC. Conversely, synoptic types 1 (38 CS) and 4 (30 CS) have low CAPE (less than 400 J/kg) and, accordingly, relatively few significant clusters of CS in relation to Corn Belt LULC. On the other hand, despite its low CAPE, synoptic type 6 has 147 CS, likely a result of associated moist low-level easterly flow over the Corn Belt. Conversely, synoptic type 7 (low to the north, high to the south) shows only 43 CS despite its moderate CAPE values, likely because of the accompanying drier westerly airflow.

The vertical motion of air over the Corn Belt can be described by the quasi-geostrophic omega (ω) equation, which relates rising and sinking air to spatial variations in vorticity and temperature advection (Bluestein 1992; Holton 2004). Because ω is calculated in terms of pressure coordinates, negative values indicate ascending motion and positive values represent sinking or subsiding air. Hence, analyses of the NARR omega fields permit an assessment of the likelihood of NCMC occurrence.

Composites of the 1000 hPa (near-surface; Fig. 10) and 500 hPa (mid-tropospheric; Fig. 11) omega fields by synoptic type support the hypothesis that the statistically significant clusters of CS around the CFB are related primarily to forcing by surface conditions, that is, differences in LULC. This contention is borne out by the patchwork average pattern of rising and sinking air noted in the 1000 hPa omega field, in contrast to the much smoother patterns in omega at the 500 hPa level. For synoptic types 3 and 5, the areas of subsidence at 500 hPa (indicated by positive omega values) are evident over large parts of the Corn Belt. However, at the near-surface (1000 hPa) level, these synoptic types show a band of rising air stretching across the fuzzy border of southern Indiana, flanked to the north and south by areas of sinking air. This pattern suggests the influence of CFBs on CS development there. The greater aerodynamic roughness of trees contrasted with crops increases the likelihood that air parcels may be forced above the local Lifted Condensation Level (LCL), particularly along and near the CFB. Under conditions of increased boundary-layer humidity—typically occurring in southerly airflow, such as synoptic types 3 and 5—the LCL will have a lower altitude than under conditions of lesser humidity (e.g., type 4). A lower LCL means that the forced air parcels are more likely to overcome CIN and realize their CAPE, with the resulting moist instability leading to CS generation.

For synoptic type 4, the omega pattern at 500 hPa is strongly positive over the Corn Belt, indicating generally subsiding air that likely explains the dearth of CS despite small patches of rising air at low levels (1000 hPa). Conversely, for synoptic type 6, rising air at 500 hPa and sinking air at 1000 hPa (producing lower tropospheric vertical

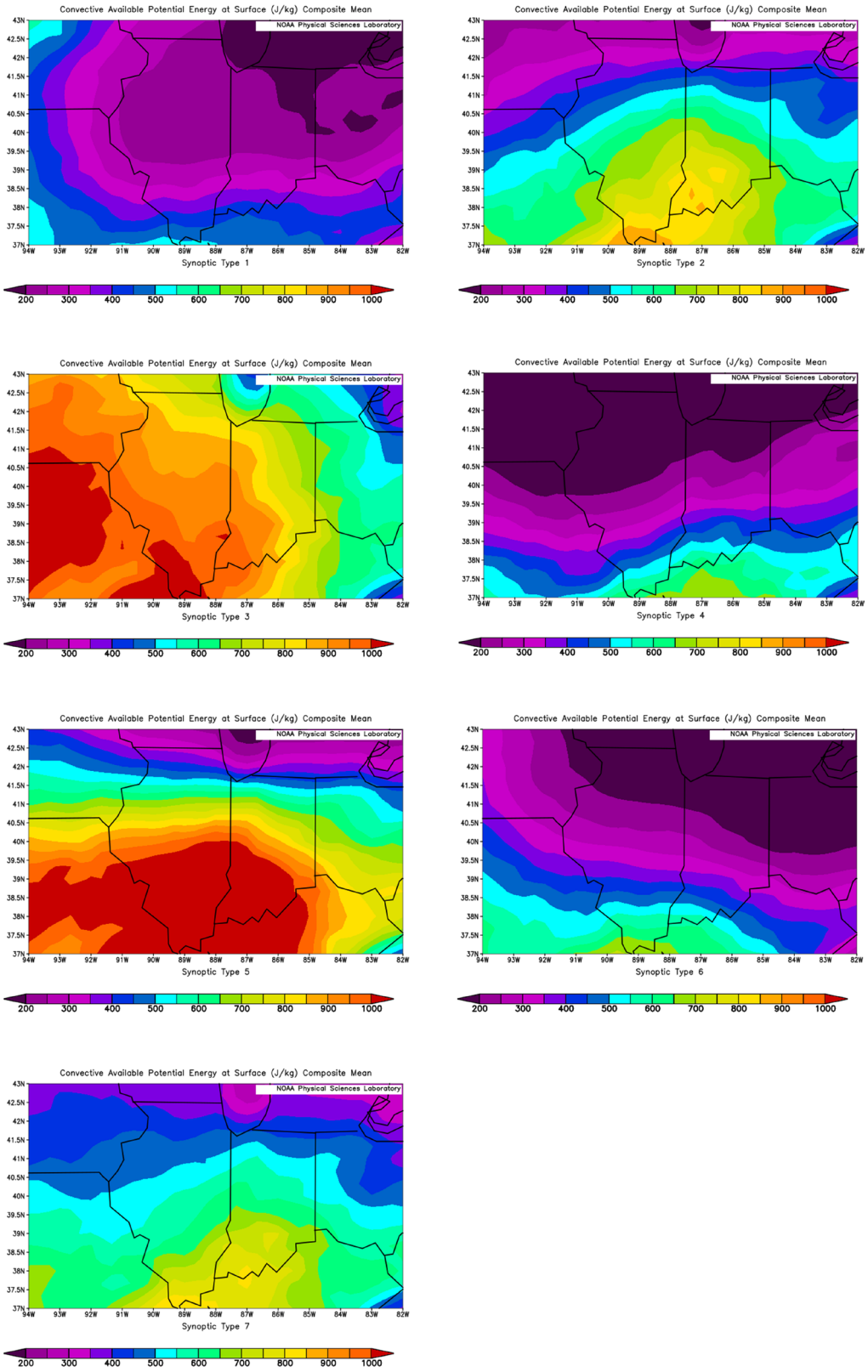

Fig. 9 Composites of the daily convective available potential energy (CAPE) for the Corn Belt by synoptic type, as described in Table 1 and 2

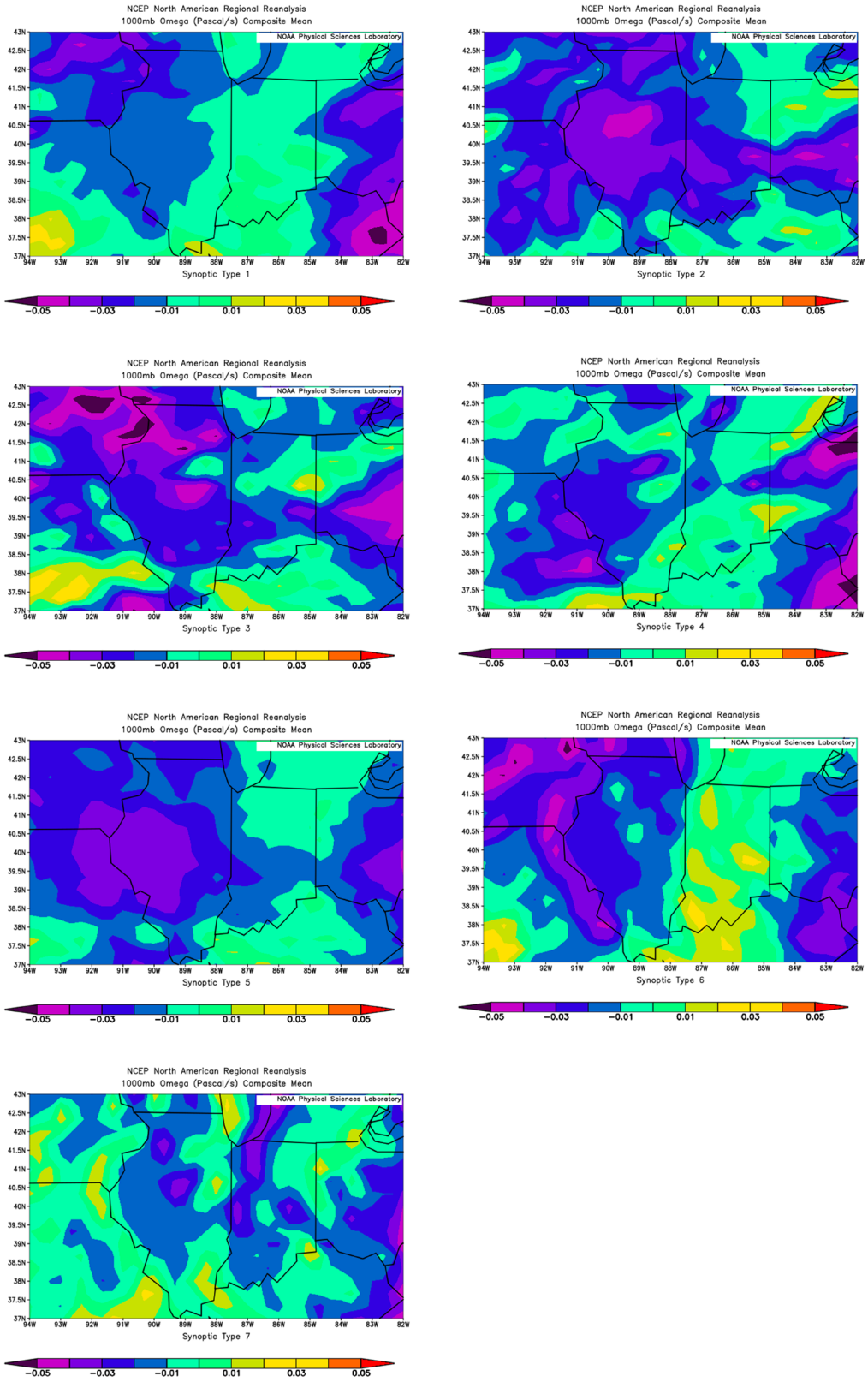

Fig. 10 Composites of the daily 1000 hPa omega (vertical motion) field for the Corn Belt, by synoptic type. Negative values indicate upward motion, while positive values indicate subsidence

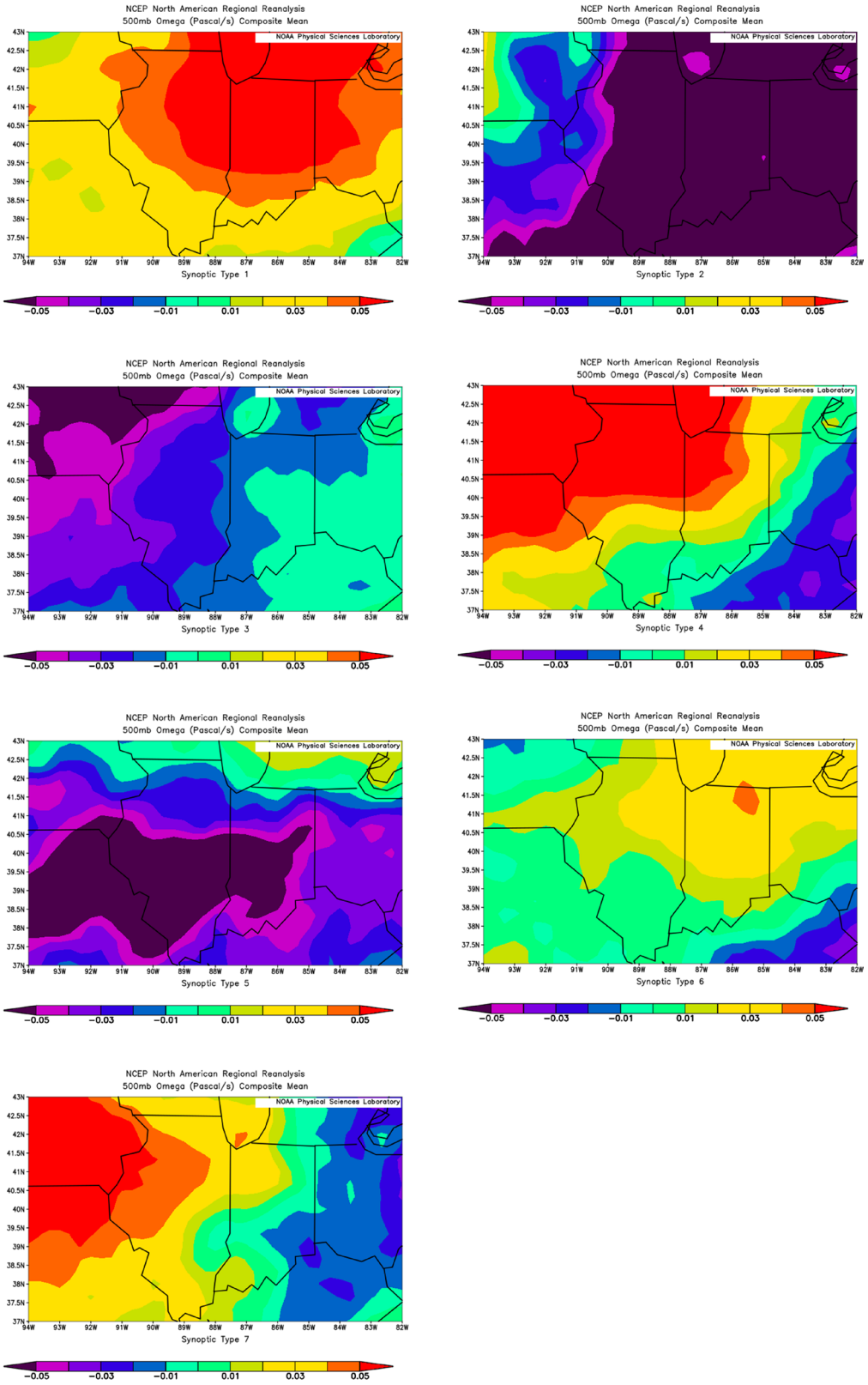

Fig. 11 Composites of the daily 500 hPa omega (vertical motion) field for the Corn Belt, by synoptic type. Negative values indicate upward motion, while positive values indicate subsidence

stretching and convergence) over Illinois (Figs. 10 and 11), suggests that CS in these synoptic types are more likely triggered by the broader circulation than by LULC. Overall, results comparing the near-surface and mid-tropospheric omega fields, stratified by synoptic type, strongly suggest that the Corn Belt LULC influences CS development—especially in the northern croplands and southeastern CFB area—occurring via an enhanced upward forcing of near-surface winds (see the 1000 hPa omega field) across a range of synoptic types. The associated fields of CAPE and 500 hPa omega are then superimposed on these surface-induced patterns, serving either to enhance (in types 3, 5, and 6) or suppress (in types 1, 4, and 7) deep convective development and CS formation. In regards to synoptic type 2, especially strong upwards vertical motion, horizontal wind-shear and upper-tropospheric divergence, would dominate the frontal deep convection, there would also be a substantial thermodynamic contribution from CAPE at and just ahead of the cold front, and an anticipated reduced influence of land surface conditions relative to types 3, 5 and 6. However, clarification of the relative importance of these forcing factors on type 2 days awaits an expanded analysis relying on a larger database.

Further evidence to support the hypothesis that the observed CS clusters may be related to NCMC formation is given by the vector wind fields on archetypal type 5 (col) days that corresponded to CS occurring over the CFB on May 7 and July 9, 2004. On these representative col days with CS development, the NARR 1000 hPa wind fields (Figs. 12a and 13a) suggest near-surface convergence in the Corn Belt. In the upper troposphere (Figs. 12b and 13b), divergence over those same areas is indicated. At upper levels, the south-to-north increase in wind speed suggests shear-induced anticyclonic vorticity and associated divergence aloft. A CS occurred over the Corn Belt in Indiana on May 7, 2004 (Fig. 12c), and three CS centered around

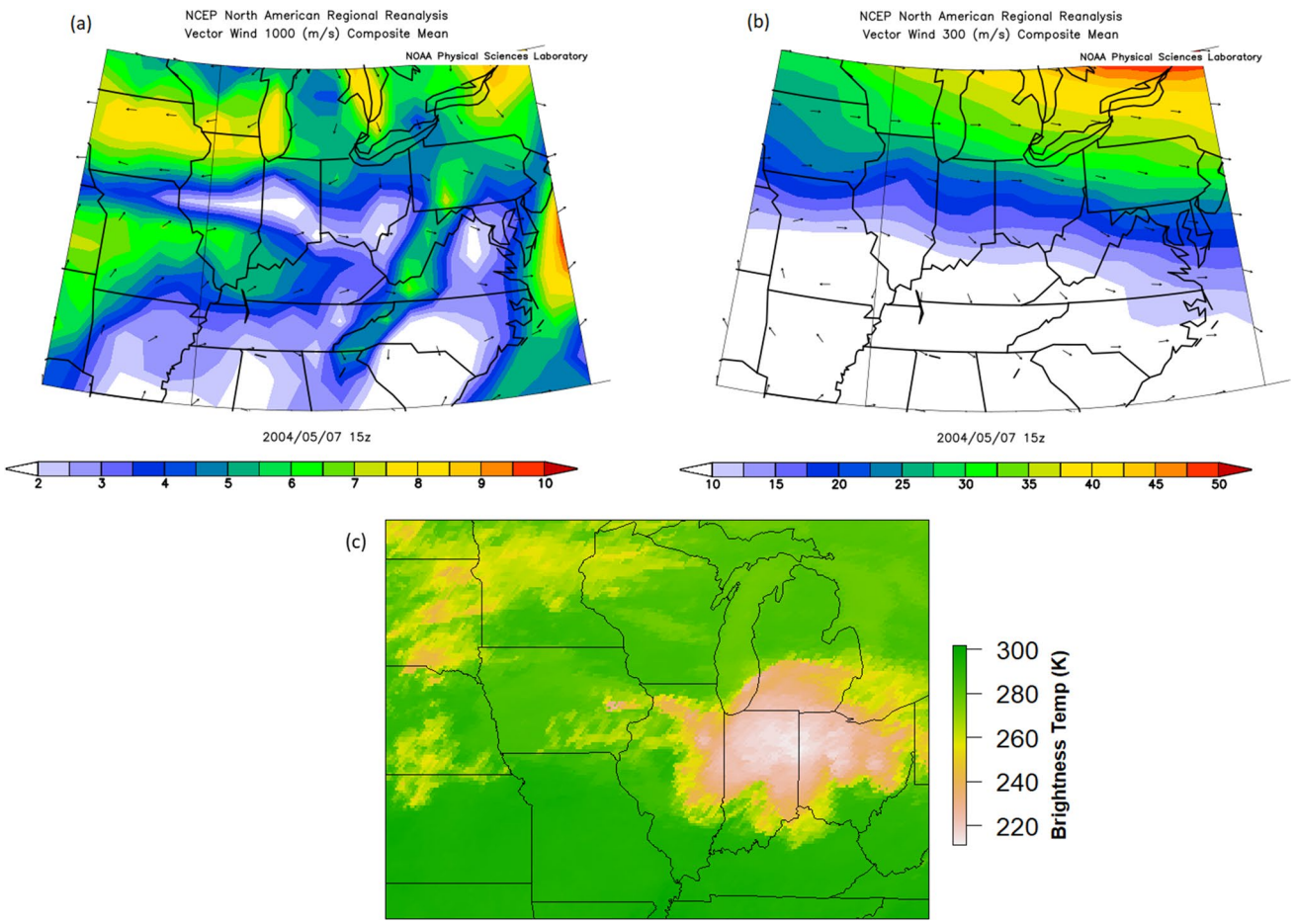

Fig. 12 NARR vector wind plots (m/s) over the Corn Belt, for **a** 1000 hPa, and **b** 300 hPa, on May 7, 2004, under synoptic type 5. **c** A false-color GOES image of the associated convective system showing the thermal IR brightness temperature (K). GOES data are from Gridsat-B1 (Knapp et al. 2011) accessed through the University of Santa Barbara's Climate Hazard Center

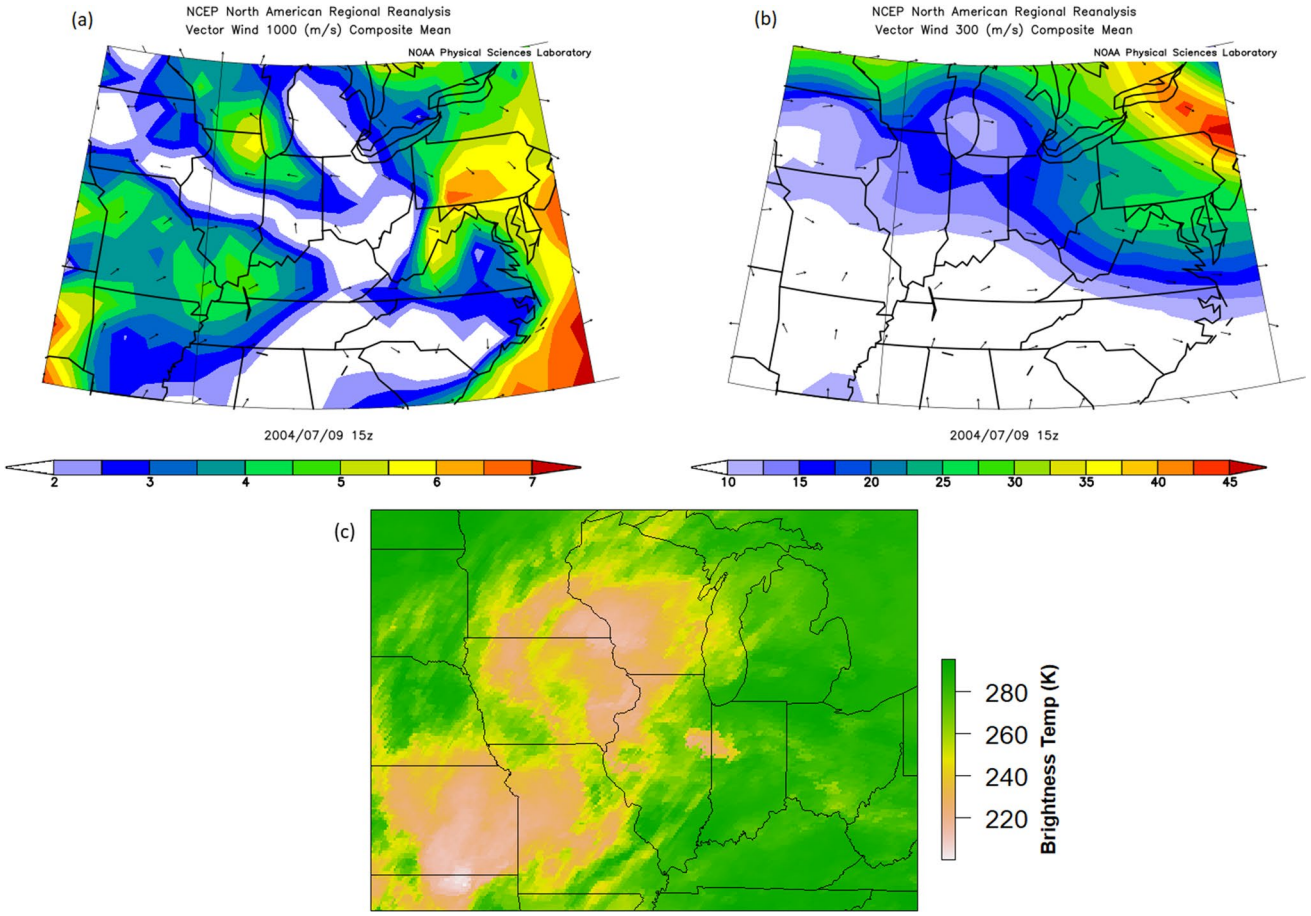

Fig. 13 NARR vector wind plots (m/s) over the Corn Belt, for **a** 1000 hPa, and **b** 300 hPa, on July 9, 2004, under synoptic type 5. **c** A false color GOES image of the associated convective system showing the thermal IR brightness temperature (K). GOES data are obtained Gridsat-B1 (Knapp et al. 2011) accessed through the University of Santa Barbara's Climate Hazard Center

the CFB in north-central Missouri occurred on July 9, 2004 (Fig. 13c). These CS, accompanying two examples of the col synoptic type, represent candidate cases suitable for detailed analysis in modeling experiments to determine more precisely the mechanisms of interaction between the land surface (LULC, soil moisture, phenology, topography) and CS development in the Corn Belt.

4 Conclusions

Spatial statistical analyses of the distributions of growing-season convective systems (CS) in relation to US Corn Belt LULC are undertaken using the ISCCP's DCTD and vegetated LULC (cropland, forest, CFB) from the NCLD. The LULC data for 1999–2007 are processed using a fuzzy map algorithm and then combined with the CS data for cluster analysis with local Moran's I. The cluster analysis reveals two main Corn Belt sub-regions of significant clustering in CS that remain relatively consistent across the start, middle, and end periods of the Corn Belt growing season. These clusters generally form in (1) the northern croplands and (2) the southeastern CFBs. This result supports our first hypothesis, that CS tend to cluster around CFBs where horizontal contrasts in heat fluxes and aerodynamic roughness are maximized. However, there is a decrease in the total number of CS through the growing season. This temporal decrease in CS, along with the differences in frequency of CS between analyzed synoptic and airflow types, supports our second hypothesis that CS development at CFBs is influenced by both vegetation phenology and synoptic patterns.

Composite results from NARR support our third hypothesis that some of the observed CS are associated with NCMC development. Concurrent patterns of CAPE and free-atmosphere (here, 500 hPa) omega—vertical motion—confirm the roles of surface heating and convective instability accompanying different synoptic types in CS development. For example, high instability and upward vertical motion support CS development in synoptic type 3, while relative stability and sinking air suppress CS development in synoptic

type 4. Visual comparison of the composite near-surface (1000 hPa) omega fields by synoptic type further supports the hypothesized influence of LULC on CS development through enhanced near-surface vertical motion of air around CFBs, possibly resulting from a combination of heat flux and aerodynamic roughness differences, even when the mid-tropospheric conditions are unfavorable (e.g., synoptic type 6). For dates that are representative of the col (saddle) synoptic type 5, the near-surface convergence of air around CFBs is accompanied by mid-troposphere divergence and anticyclonic vorticity.

Given these empirical results on interannual and sub-seasonal time scales, our future work will undertake numerical experiments using the Weather Research and Forecasting (WRF) model (Powers et al. 2017) to confirm the implied physical mechanisms producing the significant clusters of CS over the CFBs and agricultural areas within the Corn Belt. In particular, we will investigate the possible presence of NCMCs near CFBs and the possible role of aerodynamic roughness of trees (forests, CFB) versus crops in lofting air parcels above the LCL where CAPE can be realized to support deep convection (Carleton et al. 2008b). Subsequent studies will employ the WRF model in a series of experiments to establish causal relationships between CFBs and CS development in the Corn Belt. These modeling experiments will focus on determining how the spatial differences in latent heat flux, sensible heat flux, albedo, and surface roughness between croplands and remnant forests contribute to CS development, while also ruling out any potential influences of topography. Furthermore, additional modeling studies will consider inter-annual and sub-seasonal variability in LULC as expressed in NDVI or soil moisture, and how these surface characteristics may affect CS development near and along the CFBs in the Corn Belt.

Author contributions All authors contributed to the study conception and design. Material preparation, data collection and analysis were performed by Mikael Hiestand. The first draft of the manuscript was written by Mikael Hiestand and all authors commented on previous versions of the manuscript. Andrew Carleton contributed to the conceptual development and writing of the final paper. Guido Cervone contributed to developing the R code used in the statistical analysis. All authors read and approved the final manuscript

Data availability The GOES images from Gridsat B1 were access and through the University of Santa Barbara's Climate Hazard Center. All other datasets used in this study are publicly available and free to access online.

Declarations

Competing interests The authors declare no competing interests.

Competing interest The authors declare no competing interests.

References

Adegoke JO, Carleton AM (2002) Relations between soil moisture and satellite vegetation indices in the U.S. Corn Belt J Hydrometeorol 3:395–405. https://doi.org/10.1175/1525-7541(2002)003%3c0395:RBSMAS%3e2.0.CO;2

Adegoke JO, Pielke R, Carleton AM (2007) Observational and modeling studies of the impacts of agriculture-related land use change on planetary boundary layer processes in the central U.S. Agric For Meteorol 142:203–215. https://doi.org/10.1016/j.agrformet.2006.07.013

Alfieri L, Claps P, D'Odorico P, Laio F, Over TM (2008) An analysis of the soil moisture feedback on convective and stratiform precipitation. J Hydrometeorol 9:280–291

Allard J, Carleton AM (2010) Mesoscale associations between midwest land surface properties and convective cloud development in the warm season. Phys Climatol Cl 32:107–136. https://doi.org/10.2747/0272-3646.31.2.107

Anselin L (1995) Local indicators of spatial association—LISA. Geogr Anal 27:93–115. https://doi.org/10.1111/j.1538-4632.1995.tb00338.x

Anthes RA (1984) Enhancement of convective precipitation by mesoscale variations in vegetative coverin in semiarid regions. J Clim Appl Meteorol 23:541–554. https://doi.org/10.1175/1520-0450(1984)023%3c0541:EOCPBM%3e2.0.CO;2

Avissar R, Schmidt T (1998) An evaluation of the scale at which ground-surface heat flux patchiness affects the convective boundary layer using large-eddy simulations. J Atmos Sci 55:2666–2689. https://doi.org/10.1175/1520-0469(1998)055%3c2666:AEOTSA%3e2.0.CO;2

Blanchard DO (1998) Assessing the vertical distribution of convective available potential energy. Weather Forecast 13:870–877. https://doi.org/10.1175/1520-0434(1998)013%3c0870:ATVDOC%3e2.0.CO;2

Bluestein HB (1992) Principles of kinematics and dynamics. Vol. I. Synoptic-Dynamic Meteorology in Midlatitudes. Oxford University Press, New York

Blyth EM, Dolman AJ, Noilhan J (1994) The effect of forest on mesoscale rainfall: an example from HAPEX-MOBILHY. J Appl Meteorol 33:445–454. https://doi.org/10.1175/1520-0450(1994)033%3c0445:TEOFOM%3e2.0.CO;2

Brown ME, Arnold DL (1998) Land-surface–atmosphere interactions associated with deep convection in Illinois. Int J Climatol 18:1637–1653. https://doi.org/10.1002/(SICI)1097-0088(199812)18:15%3c1637::AID-JOC336%3e3.0.CO;2-U

Carleton AM, O'Neal M (1995) Satellite-derived land surface climate 'signal' for the midwest U.S.A. Int J Remote Sens 16:3195–3202. https://doi.org/10.1080/01431169508954623

Carleton AM, Travis DL, Arnold D, Brinegar R, Jelinski DE, Easterling DR (1994) Climatic-scale vegetation—cloud interactions during drought using satellite data. Int J Climatol 14:593–623. https://doi.org/10.1002/joc.3370140602

Carleton AM, Adegoke J, Allard J, Arnold DL, Travis DJ (2001) Summer season land covar - convective cloud associations fore the Midwest U.S. "Corn Belt." Geophys Res Lett 28:1679–1682. https://doi.org/10.1029/2000GL012635

Carleton AM, Arnold DL, Travis DJ, Curran S, Adegoke JO (2008) Synoptic circulation and land surface influences on convection in the midwest U.S. "corn belt" during the summers of 1999 and 2000. Part I: Composite synoptic environments. J Clim 21:3389–3415. https://doi.org/10.1175/2007JCLI1578.1

Carleton AM, Travis DJ, Adegoke JO, Arnold DL, Curran S (2008) Synoptic circulation and land surface influences on convection in the Midwest U.S. "Corn Belt" during the summers of 1999 and 2000. Part II: Role of vegetation boundaries. J Clim 21:3617–3641. https://doi.org/10.1175/2007JCLI1584.1

Chapman CJ, Carleton AM (2021) Soil moisture influence on warm-season convective precipitation for the U.S. Corn Belt J Appl Meteorol Climatol 60:1615–1632. https://doi.org/10.1175/jamc-d-20-0285.1

Collow TW, Robock A, Wu W (2014) Influences of soil moisture and vegetation on convective precipitation forecasts over the United States Great Plains. J Geophys Res Atmos 119:9338–9358. https://doi.org/10.1002/2014JD021454

Ford TW, Quiring SM, Frauenfeld OW, Rapp AD (2015) Synoptic conditions related to soil moisture-atmosphere interactions and unorganized convection in Oklahoma. J Geophys Res Atmos 120:519–535. https://doi.org/10.1002/2015JD023975

Frye JD, Mote TL (2010) Convection initiation along soil moisture boundaries in the southern Great Plains. Mon Weather Rev 138:1140–1151. https://doi.org/10.1175/2009MWR2865.1

Garcia-Carreras L, Parker DJ, Marsham JH (2011) What is the mechanism for the modification of convective cloud distributions by land surface–induced flows? J Atmos Sci 68:619–634. https://doi.org/10.1175/2010JAS3604.1

Garcia-Carreras L., Parker DJ, Taylor CM, Reeves CE, Murphy JG (2010) Impact of mesoscale vegetation heterogeneities on the dynamical and thermodynamic properties of the planetary boundary layer. J Geophys Res Atmos 115. https://doi.org/10.1029/2009JD012811

Gerken T, Bromley GT, Stoy PC (2018) Surface moistening trends in the northern North American Great Plains increase the likelihood of convective initiation. J Hydrometeorol 19:227–244. https://doi.org/10.1175/JHM-D-17-0117.1

Gerken T, Bromley GT, Ruddell BL, Williams S, Stoy PC (2018) Convective suppression before and during the United States Northern Great Plains flash drought of 2017. Hydrol Earth Syst Sci 22:4155–4163. https://doi.org/10.5194/hess-22-4155-2018

Getis A, Ord JK (1992) The analysis of spatial association by use of distance statistics. Geogr Anal 24:189–206. https://doi.org/10.1111/j.1538-4632.1992.tb00261.x

Hiestand MP, Carleton AM (2020) Growing season synoptic and phenological controls on heat fluxes over forest and cropland sites in the Midwest U.S. Corn Belt. J Appl Meteorol Climatol 53:381–400. https://doi.org/10.1175/JAMC-D-19-0019.1

Hiestand MP, Carleton AM, Davis KJ (2023) Interannual, sub-seasonal and spatial variations in growing season surface heat fluxes for the U.S. Corn Belt. Agric For Meteorol 332. https://doi.org/10.1016/j.agrformet.2023.109377

Hoerling M, Eischeid J, Kumar A, Leung R, Mariotti A, Mo K, Schubert S, Seager R (2014) Causes and predictability of the 2012 Great Plains drought. Bull Am Meteorol Soc 95:269–282. https://doi.org/10.1175/BAMS-D-13-00055.1

Holton JR (2004) An introduction to dynamic meteorology, 4th edn. Elsevier, Burlington

Huang Y, Meng Z, Zhan M (2022) Synoptic impacts on the occurrence of mesoscale boundaries and their associated convection over an area of sharp vegetation contrast. Geophys Res Let 49:e2022GL099449. https://doi.org/10.1029/2022GL099449

Huber D, Mechem D, Brunsell N (2014) The effects of Great Plains irrigation on the surface energy balance, regional circulation, and precipitation. Climate 2:103–128. https://doi.org/10.3390/cli2020103

Jin S, Homer C, Yang L, Danielson P, Dewitz J, Li C, Zhu Z, Xian G, Howard D (2019) Overall methodology design for the United States national land cover database 2016 products. Remote Sens 11. https://doi.org/10.3390/rs11242971

Kang SL, Davis KJ (2008) The effects of mesoscale surface heterogeneity on the fair-weather convective atmospheric boundary layer. J Atmos Sci 65:3197–3213. https://doi.org/10.1175/2008JAS2390.1

Knapp KR, Ansari S, Bain CL, Bourassa MA, Dickinson MJ, Funk C, Helms CN, C. C. Hennon CC, Holmes CD, Huffman GJ, Kossin JP, Lee HT, Loew A, Magnusdottir G (2011) Globally gridded satellite (GridSat) observations for climate studies. Bull Am Meteorol Soc 92:893-907. https://doi.org/10.1175/2011BAMS3039.1

Lee JM, Zhang Y, Klein SA (2019) The effect of land surface heterogeneity and background wind on shallow cumulus clouds and the transition to deeper convection. J Atmos Sci 76:401–419. https://doi.org/10.1175/JAS-D-18-0196.1

Machado LAT, Desbois M, Duvel JP (1992) Structural characteristics of deep convective systems over Tropical Africa and the Atlantic Ocean. Mon Weather Rev 120:392–406. https://doi.org/10.1175/1520-0493(1992)120%3c0392:SCODCS%3e2.0.CO;2

Machado LAT, Rossow WB, Guedes RL, Walker AW (1998) Life cycle variations of mesoscale convective systems over the Americas. Mon Weather Rev 126:1630–1654. https://doi.org/10.1175/1520-0493(1998)126%3c1630:LCVOMC%3e2.0.CO;2

Matyas CJ, Carleton AM (2010) Surface radar-derived convective rainfall associations with Midwest US land surface conditions in summer seasons 1999 and 2000. Theor Appl Climatol 99:315–330. https://doi.org/10.1007/s00704-009-0144-7

McHugh ML (2013) The chi-square test of independence. Biochem Medica 23:143–149. https://doi.org/10.11613/2FBM.2013.018

McPherson RA (2007) A review of vegetation—atmosphere interactions and their influences on mesoscale phenomena. Prog Phys Geogr 31:261–285. https://doi.org/10.1177/0309133307079055

Mesinger F, DiMego G, Kalnay E et al (2006) North American regional reanalysis. Bull Am Meteorol Soc 87:343–360. https://doi.org/10.1175/BAMS-87-3-343

Myoung B, Nielsen-Gammon JW (2010) The convective instability pathway to warm season drought in Texas. Part I: the role of convective inhibition and its modulation by soil moisture. J Clim 23:4461–4473. https://doi.org/10.1175/2010JCLI2946.1

Park S, Park SK, Lee JW, Park Y (2018) Geostatistical assessment of warm-season precipitation observations in Korea based on the composite precipitation and satellite water vapor data. Hydrol Earth Syst Sci 22:3435–3452. https://doi.org/10.5194/hess-22-3435-2018

Pielke RAS (2001) Influence of the spatial distribution of vegetation and soils on the prediction of cumulus convective rainfall. Rev Geophys 39:151–177. https://doi.org/10.1029/1999RG000072

Powers JG, Klemp JB, Skamarock WC, Davis CA, Dudhia J, Gil DO, Coen JL, Gochis DJ, Ahmadov R, Peckham SE, Grell GA (2017) The weather research and forecasting model: Overview, system efforts, and future directions. Bull Am Meteorol Soc 98:1717–1737. https://doi.org/10.1175/BAMS-D-15-00308.1

Rabin RM, Stadler S, Wetzel PJ, Stensrud DJ, Gregory M (1990) Observed effects of landscape on convective clouds. Bull Am Meteorol Soc 71:272–280. https://doi.org/10.1175/1520-0477(1990)071%3c0272:OEOLVO%3e2.0.CO;2

Rossi F, Becker G (2019) Creating forest management units with hot spot analysis (Getis-Ord Gi*) over a forest affected by mixed-severity fires. Aust For 82:166–175. https://doi.org/10.1080/00049158.2019.1678714

Rossow WB, Garder LC (1993) Cloud detection using satellite measurements of Infrared and Visible Radiences for ISCCP. J Clim 6:2341–2369. https://doi.org/10.1175/1520-0442(1993)006%3c2341:CDUSMO%3e2.0.CO;2

Rossow WB, Knapp KR, Young AH (2022) International satellite cloud climatology project: Extending the record. J Climate 35:141–158. https://doi.org/10.1175/JCLI-D-21-0157.1

Roy SB, Avissar R (2002) Impact of land use/land cover change on regional hydrometeorology in Amazonia. J Geophy Res Atmos 107: LBA 4–1-LBA 4–1210.1029/2000JD000266

Schiffer RA, Rossow WB (1983) The international satellite cloud climatology project (ISCCP): the first project of the world climate research programme. Bull Am Meteorol Soc 64:779–784. https://doi.org/10.1175/1520-0477-64.7.779

Schiffer RA, Rossow WB (1985) ISCCP global radiance data set: a new resource for climate research. Bull Am Meteorol Soc 66:1498–1505. https://doi.org/10.1175/1520-0477(1985)066%3c1498:igrdsa%3e2.0.co;2

Segal M, Arritt RW (1992) Nonclassical mesoscale circulations caused by surface sensible heat- flux gradients. Bull Am Meteorol Soc 73:1593–1604. https://doi.org/10.1175/1520-0477(1992)073%3c1593:NMCCBS%3e2.0.CO;2

Segal M, Aviara R, McCumber MC, Pielke RA (1988) Evaluation of vegetation effects on the generation and modification of mesoscale circulations. J Atmos Sci 45:2268–2293. https://doi.org/10.1175/1520-0469(1988)045%3c2268:EOVEOT%3e2.0.CO;2

Taylor CM, Parker DJ, Harris PP (2007) An observational case study of mesoscale atmospheric circulations induced by soil moisture. Geophys Res Lett 34. https://doi.org/10.1029/2007GL030572

Trapp RJ (2013) Mesoscale-convective processes in the atmosphere. Cambridge University Press, New York

Weaver CP (2004) Coupling between large-scale atmospheric processes and mesoscale land–atmosphere interactions in the US Southern Great Plains during summer. Part I: Case Studies. J Hydrometeorol 5:1223–1246. https://doi.org/10.1175/JHM-396.1

Xie Y, Sha Z, Yu M (2008) Remote sensing imagery in vegetation mapping: a review. J Plant Ecol 1:9–23. https://doi.org/10.1093/jpe/rtm005

Yang L, Jin S, Danielson P, Homer C, Gass L, Bender SM, Case A, Costello C, Dewitz J, Fry J, Funk M (2018) A new generation of the United States National Land Cover Database: requirements, research priorities, design, and implementation strategies. ISPRS J Photogramm Remote Sens 1:108–123. https://doi.org/10.1016/j.isprsjprs.2018.09.006